CHAPTER IV

GEOTHERMOBAROMETRY

4.1 Introduction

The aims of this chapter are (1) to determine geothermobarometric conditions of the host basaltic melts before erupting to the surface and (2) to estimate the last equilibrium P-T conditions of the deep-seated xenoliths. Therefore, some suitable samples were selected for thermobarometric study. Most of the selected xenoliths are apparently high-grade metamorphic varieties formed under severe plastic deformation, as indicated by recrystallized plagioclase matrix wrapping around partially recrystallized, augen-shaped porphyroblast aggregates as well as curved cleavage traces of clinopyroxene. These deformations were seemingly generated under a lower crust - upper mantle condition.

For the host basalts, a few geothermobarometric models, based on clinopyroxene- and olivine-basalt equilibria, are suitable for this study. The phenocrysts observed in basalts are mostly olivine, with subordinated clinopyroxe, whereas orthopyroxene and plagioclase phenocrysts are either rare or absent. Clinonopyroxene-liquid equilibria of Putirka *et al.* (1996 and 2003) and olivine-liquid equilibria of Putirka *et al.* (2007) were selected because they have yielded the best fit constraints compared to other available models, e.g. Helz and Thornber (1987), Sisson and Grove (1992), Beattie (1993), Nimis (1995), Nimis and Ulmer (1999), Nimis and Taylor (2000). Pressure (P) and temperature (T) estimation of these geothermobarometric models has been done using MS Excel spreadsheets that are available on Putirka's homepage (www.csufresno.edu/ees/Faculty&Staff/ Putirka/Keith_Putirka.html).

For the xenoliths, several equilibrium reactions among end-member components of crucial coexisting phases have been thermodynamically calibrated and utilized as thermobarometers. The calculations were performed through PET and PeRpLeX. Both packages provide a wide range of thermodynamic database.

PET is a set of free programs developed as a Mathematica®-based package by combining features of several petrological programs, for instance, MINTAB (Rock and Caroll, 1990) TWQ (Berman 1991), THERMOCALC (Holland and Powell, 1991), PTMAFIC (Soto and Soto, 1995), PTOXY (Nashir, 1994), THERMOBAROMETRY (Spear *et al.*, 1991), etc., into the package (Dachs, 1998; 2004). This package is available on www.uni-salzburg.at/portal/page? pageid=805.259394&dad=portal& schema=PORTAL. Mathematica® program, up to version 7.0, is needed to be installed prior to run PET. In this study, this program package was used to perform geothermobarometric estimation based on various single equilibria related to mineral chemistry data as input and then illustration is generated as graphical P-T diagram.

PeRpLeX is a collection of program packages developed for calculating phase diagrams and equilibria which can be run on Windows, Mac, Os, X and Linux. It provides simple estimation of rock and mineral properties as a function of pressure, temperature and/or composition (Connolly and Kerrick, 1987; Connolly, 1990). This program package is a freeware and ready to use; it can be downloaded from www.perplex.ethz.ch/perplex.html. In this study, PeRpLeX was engaged to create pseudosection of all possible equilibrium fields among mineral phases based on whole-rock chemical composition of the xenoliths. The obtained results from PeRpLeX are also used as a recheck tool for validation of P-T conditions derived from PET calculation whether they are consistent with the mineral assemblages petrographically observed.

4.2 Geothermobarometry of Basalts

As aforementioned, geothermometers, based on clinopyroxene-basalt and olivine-basalt equilibria, were applied for estimating P-T conditions of the basalt specimens collected from three different basaltic units of the study area. The clinopyroxene-basalt equilibrium may provide P-T constraints of the basaltic magmas. Various compositions of clinopyroxene phenocrysts have been obtained

from EPMA; they are assumed to have been crystallized continuously during the processes of basaltic melting and rising to the surface. Therefore, basaltic magma, extremely enormous, has relatively unchanged in comparison with tiny clinopyroxene phenocrysts. Moreover, olivine-basalt thermometry could be carried out by applying pressures which may be estimated from the previous equilibria.

Clinopyroxene-Basalt Thermobarometry: Putirka *et al.* (1996) proposed a thermobarometer for mafic igneous rocks based on clinopyroxene-liquid equilibria. They incorporated their experimental results with the existing published data to calibrate such a geothermobarometer. Using various mafic bulk compositions, the experiments were set from 8-30 kb and 1100–1475ºC. The calibrations for a geothermometer were based on partitioning of the jadeite (Jd; $NaAlSi_2O_6$) and diopside-hedenbergite (DiHd; $Ca(Mg,Fe)Si_2O_6$) components between clinopyroxene and liquid, which is temperature sensitive. The equilibrium constant for jadeite component was used on a basis of geobarometer due to its more sensitivity toward pressure. The proposed geothermobarometer expressions are:

$$\frac{10^4}{T(ºK)} = 6.73 - 0.26 \ln \frac{Jd^{cpx} Ca^{liq} Fm^{liq}}{DiHd^{cpx} Na^{liq} Al^{liq}} - 0.86 \ln \frac{Mg^{liq}}{Mg^{liq} + Fe^{liq}} + 0.52 \ln Ca^{liq}$$

and

$$P(kbar) = -54.3 + 299 \frac{T(ºK)}{10^4} + 36.4 \frac{T(ºK)}{10^4} \ln \frac{Jd^{cpx}}{(Si^{liq})^2 Na^{liq} Al^{liq}} + 367 Na^{liq} Al^{liq}$$

On the same basis of clinopyroxene-liquid equilibria, Putirka *et al.* (2003) improved and expanded their prior model to be suitable for wider compositions from mafic melts to SiO_2-rich liquids (up to 71.3 wt % SiO_2). These revised geothermobarometer expressions are:

$$\frac{10^4}{T(°K)} = 4.6 - 0.437 \ln \frac{Jd^{cpx} \, Ca^{liq} \, Fm^{liq}}{DiHd^{cpx} \, Na^{liq} \, Al^{liq}} - 0.654 \ln Mg'^{liq} - 0.326 \ln Na^{liq}$$

$$- \, 6.32 \times 10^{-3} \, P(kbar) - 0.92 \ln Si^{liq} + 0.274 \ln Jd^{px}$$

and

$$P(kbar) = - \, 88.3 + 2.82 \times 10^{-3} \, T(°K) \ln \frac{Jd^{cpx}}{(Si^{liq})^2 \, Na^{liq} \, Al^{liq}} + 2.19 \times 10^{-2} \, T(°K)$$

$$- \, 25.1 \ln Ca^{liq} \, Si^{liq} + 7.03 \, Mg'^{liq} + 12.4 \ln Ca^{liq}$$

Here, Jd^{cpx} is the mole fraction of jadeite and $DiHd^{cpx}$ is the mole fraction of diposide + hedenbergite in clinopyroxene, where pyroxene cations are calculated on the basis of 6 oxygen atoms. The Jd component is the lesser Na or Al^{vi} and the remaining Al is used to form CaTs. The DiHd component is calculated as the fraction of Ca remaining after forming Ca-tschermak ($CaAl_2Si_2O_6$; CaTs = Al^{vi} - Jd), $CaTiAl_2O_6$ (= (Al^{iv} - CaTs)/2) and $CaCr_2SiO_6$ (= Cr/2). Si^{liq}, Al^{liq}, Ca^{liq}, Na^{liq}, Mg^{liq} and Fe^{liq} are cation fractions in the liquid recalculated to a 6 oxygen formula unit. Fm^{liq} is the sum of MgO^{liq} and FeO^{liq} and Mg'^{liq} is the cation fraction ratio of $MgO^{liq}/(MgO^{liq} + FeO^{liq})$. The standard errors of estimates are about 0.3 kb and 30°K for the 1996 model and about 1.7 kb and 33°K for the 2003 model. For this study, the liquid compositions are from whole-rock analyses of basalts (see Table 2.1) and the clinopyroxene compositions are core compositions of individual clinopyroxene phenocrysts obtained from EPMA analyses (see Table 2.4). The valid temperatures and pressures given by the clinopyroxene-basalt thermobarometry from 9 samples (70 phenocrysts), including *KNg02* (10 grains), *KKYd02* (5 grains), *KKYd04* (9 grains), *KKMb02* (7 grains), *KKNt02* (14 grains), *KKNt04* (11 grains), *KOk01* (1 grain), *KKb01* (12 grains) and *KKb03* (1 grain), are displayed in Tables 4.1 and 4.2.

Results: The overall temperature and pressure ranges of the studied basalts are quite consistent for all specimens (Figure 4.1). The Ngulai basalts yield the widest ranges of temperatures and pressures from ~1,200-1,450°C and 6-27 kb

Table 4.1 Estimated P-T of basaltic magmas using the clinopyroxene-melt thermobarometer of Putirka et al. (1996).

*Moho depth: ~ 40-44 km
*Lower Crust : ~ 20 km-thick

Nguu Basalts

KNg02: 10 Cpx phenocrysts

T(°C) 1453	1391	1378	1378	1370	1351	1347	1311	1259	1191
P(kb) 29	23	22	22	21	19	19	15	9	2
Depth (km)** 94	76	72	72	69	63	62	50	31	7

Ngulai Basalts

KKYd02: 5 Cpx phenocrysts

T(°C)	P(kb)	Depth (km)**
1446	25	84
1349	18	59
1330	16	52
1323	15	51
1314	14	47

Ngulai Basalts

KKYd04: 9 Cpx phenocrysts

T(°C) 1372	1377	1366	1355	1346	1345	1331	1329	1305
P(kb) 20	20	19	18	18	18	16	16	13
Depth (km)** 66	65	64	61	58	58	53	52	44

KKMb02: 7 Cpx phenocrysts

T(°C) 1384	1258	1252	1247	1229	1209	1196
P(kb) 22	9	9	8	6	4	3
Depth (km)** 72	31	29	26	20	13	9

KOk01: 1 Cpx phenocryst

T(°C)	P(kb)	Depth (km)**
1200	9	28

KKNt02: 14 Cpx phenocrysts

T(°C) 1326	1315	1307	1307	1284	1281	1269	1260	1254	1247	1241	1238	1206	1187
P(kb) 17	16	15	15	13	12	11	10	10	9	8	8	5	2
Depth (km)** 57	52	50	50	42	41	37	34	32	30	27	26	15	8

KKNt04: 11 Cpx phenocrysts

T(°C) 1246	1239	1237	1231	1228	1227	1218	1205	1203	1186	1175
P(kb) 12	12	11	11	10	10	9	8	8	6	5
Depth (km)** 41	38	37	35	34	34	31	26	25	19	15

Kiboko (Chyulu) Basalts

KKb03: 1 Cpx phenocryst

T(°C)	P(kb)	Depth (km)**
1218	8	27

KKb01: 12 Cpx phenocrysts

T(°C) 1404	1403	1402	1334	1307	1298	1266	1254	1235	1229	1183	1179
P(kb) 24	24	24	18	15	14	11	10	8	7	2	2
Depth (km)** 81	80	80	60	50	47	37	32	25	24	7	6

* According to seismic tomography studies by Novak et al. (1997) and Ritter and Kaspar (1997); **assuming 3.3 km/kb.

Table 4.2 Estimated P-T of basaltic magmas using the clinopyroxene-melt thermobarometer of Putirka *et al.* (2003).

*Moho depth: ~ 40-44 km	Nguu Basalts										Ngulai Basalts				
*Lower Crust : ~ 20 km-thick	KNg02: Cpx phenocryst										KKYd02: Cpx phenocryst				
T(°C)	1425	1378	1364	1368	1369	1346	1347	1319	1295	1244	1453	1334	1329	1314	1312
P(kb)	28	24	23	23	22	21	21	18	14	8	27	21	19	19	18
Depth (km)**	93	79	77	76	74	70	69	60	45	27	87	69	63	62	60

Ngulai Basalts

	KKYd04: Cpx phenocryst									KKMb02: Cpx phenocryst						
T(°C)	1360	1387	1356	1346	1336	1335	1328	1332	1312	1382	1291	1289	1286	1271	1256	1243
P(kb)	22	22	22	21	20	20	19	19	17	23	13	13	12	11	9	8
Depth (km)**	73	72	72	69	67	67	63	62	56	76	44	42	41	36	31	28

	KOk01: Cpx phenocryst								KKNt02: Cpx phenocryst							
T(°C)	1193		1321	1320	1309	1313	1294	1292	1285	1278	1272	1267	1261	1261	1238	1224
P(kb)	9		17	16	16	16	14	14	13	12	12	11	11	10	8	6
Depth (km)**	31		57	54	52	52	46	45	42	40	38	37	35	34	25	20

	KKNt04: Cpx phenocryst										
T(°C)	1244	1242	1240	1235	1233	1231	1226	1216	1215	1202	1195
P(kb)	11	11	11	10	10	10	9	8	8	6	5
Depth (km)**	38	36	35	34	33	33	30	27	26	21	18

Kiboko (Chyulu) Basalts

	KKb03: Cpx phenocryst	KKb01: Cpx phenocryst											
T(°C)	1201	1362	1362	1361	1306	1289	1282	1256	1255	1245	1233	1201	1198
P(kb)	11	24	24	24	19	17	16	14	13	11	11	7	7
Depth (km)**	35	79	79	79	63	56	54	46	42	37	36	23	22

* According to seismic tomography studies by Novak et al. (1997) and Ritter and Kaspar (1997); **assuming 3.3 km/kb.
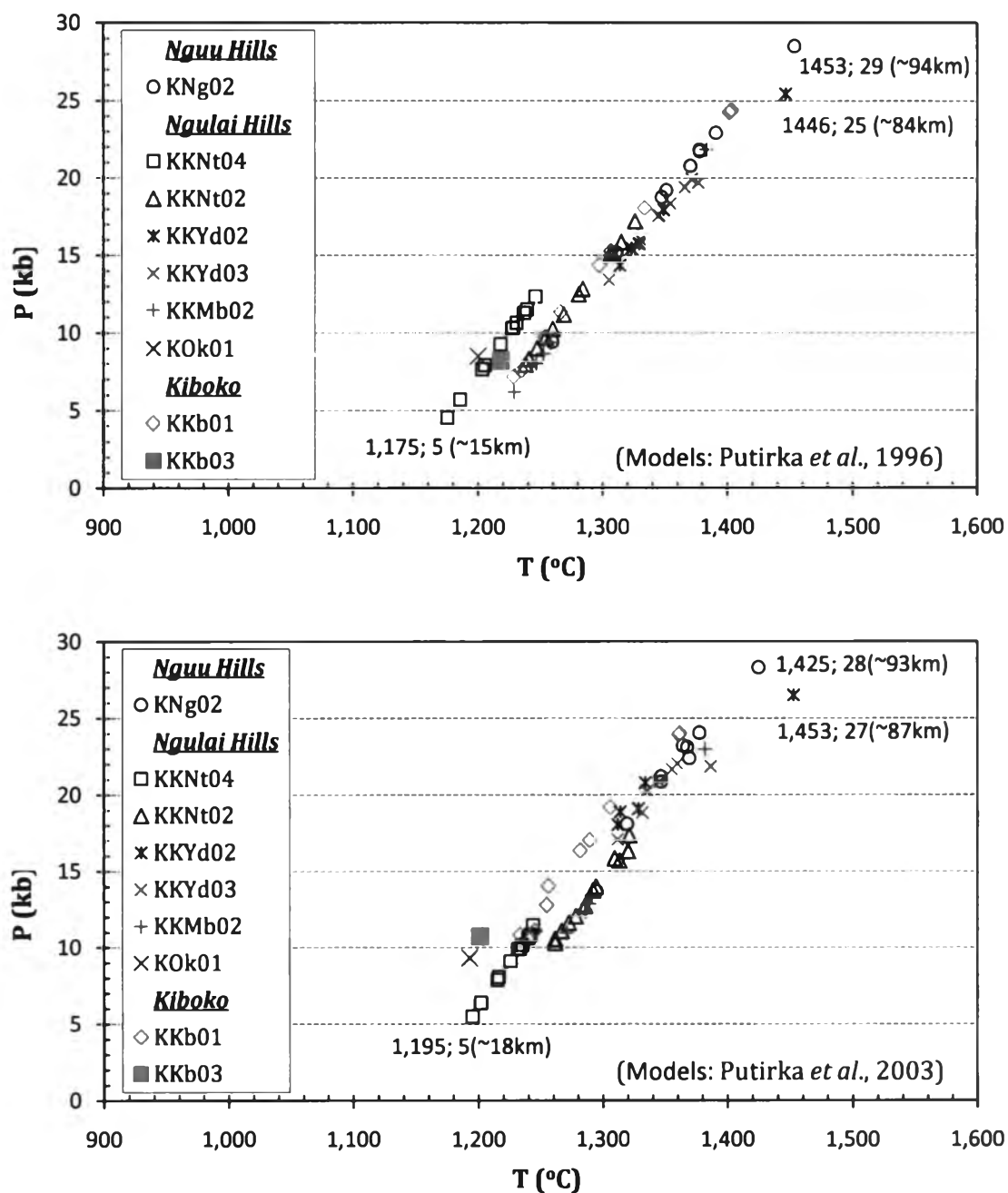
Figure 4.1 P-T diagrams of the studied basalt specimens estimated using clinopyroxene-melt thermobarometers of Putirka *et al.* (1996: top) and (2003: bottom).

covering those of the Nguu (1,240-1,425°C and 8-28 kb) and Kiboko (1,200-1,360 and 7-24 kb) basalts. Among all, some clinopyroxene phenocrysts in samples *KNg02* from the Nguu Hills and *KKYd02* from Kyanduini cone of the Ngulai Hills area were equilibrated at the highest P-T condition range of slightly exceeding 1,400°C and at

almost 30 kb (~80-90 km) following by samples *KKb01* from Kiboko vicinity southof the Nguu Hills, *KKMb02* from Kwa KMbiti cone, *KKYd04* from Kyanduini cone and *KKNt02* from Kwa Nthuku cone of the Ngulai Hills area yielded above 1,300 up to about 1,400°C in the range of 17-22 kb (~60-70 km). In *KKNt04* from Kwa Nthuku cone and *KOk01* from Ol Doinyo Orkaria cone of the Ngulai area and *KKb03* from Mwailo cone near Kiboko Agricultural Research Institute, phenocrysts appear to equilibrate with melt at T below 1250°C under a pressure range of 8-12 kb (equivalent to depth ~30-40 km). This can sequentially arrange from deeper to shallower: *KNg02 ≈ KKYd02 > KKb01 ≈ KMb02≈ KKYd02> KKNt02 > KKNt04 >* KKb03 ≈ *KOk01*.

Olivine-Basalt Thermometry: In comparison to the mineral chemistry of clinopyroxene, olivine is more suitable for thermometry because its composition has been slightly changed during the fractionation process, which is temperature dependent. Putirka *et al.*, (2005; 2007) proposed a thermometer calibrated from olivine-liquid equilibria. They also applied this thermometer for estimating the mantle potential temperatures at Hawaii, Iceland, and the mid-ocean ridge localities. For this study, this thermometer was used as a recheck tool for estimation of temperatures of the basaltic magmas resulted from the clinopyroxene-liquid thermobarometer. The proposed geothermometer expression is:

$$T(°C) = 15294.6 + 1318.8 \, P_{est}(GPa) + 2.4834 \, P_{est}(GPa)^2 \, /$$
$$\{8.048+2.8352 \ln K_d(Mg) + 2.097 \ln [1.5 \, (Mg^{liq} + Fe^{liq} + Mn^{liq} + Ca^{liq})]$$
$$+ 2.575 \ln [3 \, Si^{liq}] - 1.41 \, [3.5 \ln (1 - Al^{liq}) + 7 \ln (1 - Ti^{liq})] + 0.222 \, H_2O^{liq}(\%)$$
$$+ 0.5 \, P_{est}(GPa)\}$$

Here, P_{est} is a given value as assumed pressure in GPa unit. $K_d(Mg)$ is the cation fraction ratio of $(X_{Mg})^{ol}/(X_{Mg})^{liq}$. Si^{liq}, Al^{liq}, Ca^{liq}, Mg^{liq}, Fe^{liq} and Mn^{liq} are cation fractions in the liquid recalculated to a 6 oxygen formula unit. H_2O^{liq} is wt % LOI of liquid. For this study, the liquid compositions are from whole-rock analyses of basalts (see Table 2.1) and the selected olivine compositions are core compositions of individual olivine

phenocrysts obtained from EPMA analyses (see Table 2.4). After being calculated, all T values obtained from individual olivine phenocrysts in each sample are averaged to give a mean equilibrium T, at a given pressure, for that specimen. The maximum, minimum and average values of estimated temperatures according to the olivine-basalt thermometry from 6 samples (110 phenocrysts), including *KNg02* (18 grains), *KNg05* (34 grains), *KNg10* (8 grains), *KNg11* (30 grains), *KOk01* (2 grains) and *KKYd02* (18 grains), are displayed in Table 4.3.

Table 4.3   Ranges of temperatures at given pressures (P_{est}) estimated using the olivine-basalt thermometer of Putirka *et al.* (2007).

P_{est}(kb)	5	10	15	20	25	30	5	10	15	20	25	30
	Nguu basalts											
T (°C)	KNg05 (34 grains)						KNg10 (8 grains)					
Average	1275	1302	1327	1352	1377	1400	1382	1409	1435	1446	1484	1493
Max	1354	1381	1406	1431	1455	1479	1506	1533	1558	1582	1605	1628
Min	1247	1274	1300	1325	1349	1373	1356	1383	1409	1325	1458	1373
SD	*29.7*	*29.7*	*29.7*	*29.7*	*29.6*	*29.6*	*51.9*	*51.7*	*51.5*	*70.1*	*51.0*	*69.5*
	Nguu basalts											
T (°C)	KNg11 (30 grains)						KNg02 (18 grains)					
Average	1315	1339	1365	1390	1381	1404	1391	1423	1449	1474	1498	1521
Max	1855	1877	1898	1919	1448	1471	1426	1453	1479	1503	1527	1550
Min	1247	1274	1300	1325	1349	1372	1277	1393	1419	1444	1468	1491
SD	*134.9*	*134.4*	*133.4*	*132.3*	*20.8*	*20.8*	*33.3*	*20.4*	*20.3*	*20.2*	*20.1*	*20.0*
	Ngulai Basalts											
T (°C)	KKYd02 (18 grains)						KOk01 (2 grains)					
Average	*1376*	*1402*	*1428*	*1453*	*1477*	*1500*	*1175*	*1202*	*1228*	*1253*	*1277*	*1300*
Max	*1439*	*1465*	*1491*	*1515*	*1539*	*1562*	*1182*	*1208*	*1234*	*1259*	*1283*	*1307*
Min	*1349*	*1376*	*1402*	*1427*	*1451*	*1474*	*1169*	*1196*	*1221*	*1246*	*1270*	*1294*
SD	*21.1*	*21.0*	*20.9*	*20.9*	*20.8*	*20.7*	*8.9*	*8.9*	*8.9*	*8.9*	*9.0*	*9.0*

Results: The overall averaged temperature ranges obtained from this thermometry are equivalent to those obtained from the clinopyroxene-basalt thermobarometers. At given range of pressures from 5-30 kb, the Nguu and Ngulai basalts considerably yield the same range of average temperatures, ~1,300-1,500°C (Figure 4.2). However, each sample individually exhibits its own estimated temperature at the same levels of pressure. At given 30 kb, *KNg02* from the Nguu Hills gives the highest average temperature of ~1,500°C, whereas. *KOk01* from the Ngulai Hills has the lowest average temperature of ~1,200°C. The temperature discrepancy observed at equivalent pressure level may reversely imply that specimens were either equilibrated at various depths or derived from sources at different depth, e.g. from deeper to shallower: *KNg02 > KKYd02 ≃ KNg10 > KNg11 > KNg05 > KOk01.* This sequence also corresponds to the output yielded from the clinopyroxene-basalt thermobarometers.
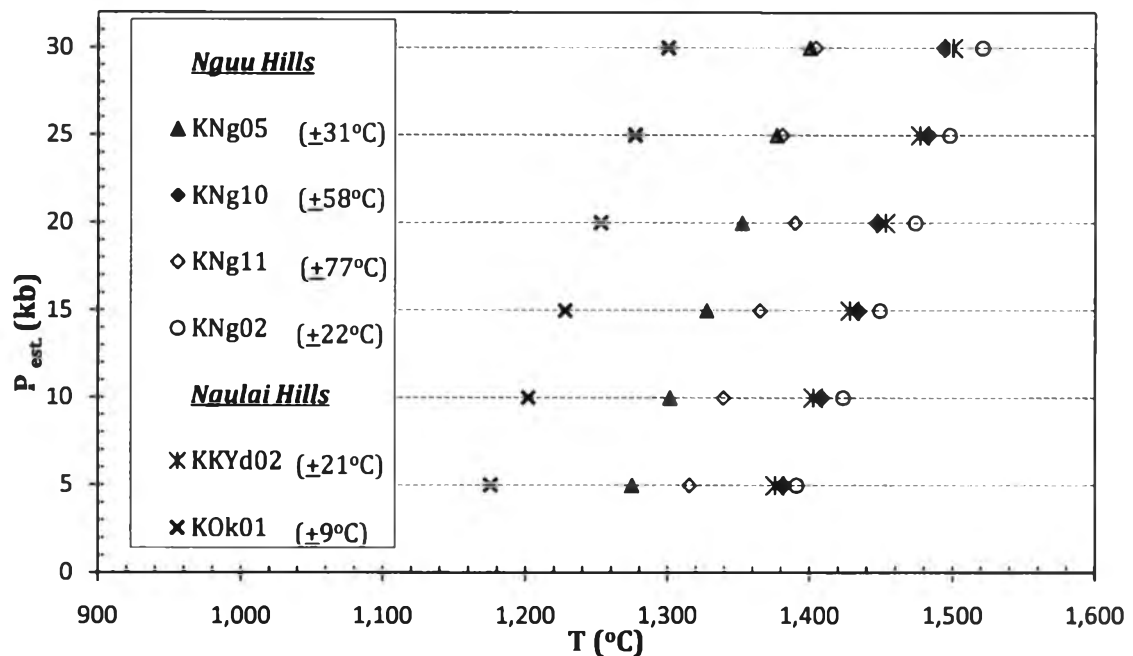
Figure 4.2 **Average temperatures of each studied basalt specimen estimated using olivine-liquid thermometer of Putirka *et al.* (2007). Blue bar inside the legend box represents approximate SD of T calculation.**

4.3 Geothermobarometry of Xenoliths

As applying PET for P-T estimation based on single equilibrium calculations, the results are summarized in Table 4.4 and P-T constraints in a graphical format of each representative specimen are also shown (Figures 4.3-4.6). An intersection between two or more geothermobarometers represents each P-T constraint point. A best-fit P-T constraint of individual samples is assumed from a point where a most geothermobarometers intersect or where the tightest spaced P-T lines between two geothermobarometers cut across each other.

Results: The mineral assemblages observed in the granulite samples, both corundum-bearing and barren type, seem to provide better P-T constaints in relative to those of the peridotite and pyroxenite samples.

Table 4.4 Summary of P-T equilibrium ranges of each xenoliths group from the Nguu and Ngulai Hills derived from intersections between thermometer and barometer of representative samples.

Xenolith group	Peridotite		Pyroxenite
Xenolith type *(Representative sample no.)*	Spl lherzotite *(Ng07)*	Wehrlite *(Ng18)*	Websterite *(Ng34)*
Thermometer/Barometer	**T(°C)/P(kb)**	**T(°C)/P(kb)**	**T(°C)/P(kb)**
Cpx-Opx/Grt-Opx	825–1,010 /9-18	750–1,000 /7-15.5	1,000–1,200 /9-22.5
Ol-Spl/Grt-Opx	875–900 /11-17	950–1,000 /10-15.5	--
Ol-Cpx/Grt-Opx	1,100–1,125 /18.5-21	1,075–1,100 /14-18.5	--
Grt-Spl/Grt-Opx	1,350-1,500/ 26-33.5	--	--
Grt-Cpx/Grt-Opx	775–960 /8.5-18.5	--	--
Best-fit P-T constraint	1,100/18.5 (~61 km)*	1,100/17.5 (~58 km)*	1,075/14.5 (~48 km)*

* assuming 3.3 km/kb

Table 4.4 (cont.).

Xenolith group	Granulite		
Xenolith type (*Representative sample no.*)	Corundum (Crn)-bearing		Crn-free
	Foliated (*KNt01*)	Banded (*Ng21*)	Non-foliated (*KMb01*)
Thermometer/Barometer	T(°C)/P(kb)	T(°C)/P(kb)	T(°C)/P(kb)
Cpx-Opx/Grt-Opx	850–975 /9.5-14.5	850–950 /10-13	750–850 /5.5-12.5
Cpx-Opx/Grt-Cpx-Pl-Qtz	875–975 /16.5-19.5	850–950 /16-19	825–875 /14-16.5
Cpx-Opx/Grt-Opx-Pl-Qtz	875–975 /13.5-16.5	850–975 /14.5-16.5	800–850 /10.5-11.5
Grt-Opx/Grt-Cpx-Pl-Qtz	1,125–1,300 /19.5-23	1,125–1,300 /19.5-23	925–1,275 /14.8-20.5
Grt-Opx/Grt-Opx-Pl-Qtz	950–1,125 /14-17.5	975–1,125 /14-17.5	800-990 /10.5-12
Grt-Cpx/Grt-Opx	800–925 /8.7-16	--	--
Grt-Cpx/Grt-Cpx-Pl-Qtz	875–975 /18.5-21	--	--
Grt-Cpx/Grt-Opx-Pl-Qtz	840–925 /14.5-18.5	--	--
Best-fit P-T constraint (Cpx-Opx/Grt-Opx/ Grt-Opx-Pl-Qtz)	1,025/16 (~53 km)*	975/14 (~46 km)*	850/11 (~36 km)*

* assuming 3.3 km/kb

Peridotite Xenoliths: The P-T constraints of this xenolith group were obtained from 2 representative samples, *Ng07* and *Ng18*, using 6 different geothermobarometers, which are (1) Grt-Cpx (Berman *et al.*, 1995), (2)Cpx-Opx (Brey and Köhler, 1990), (3) Ol-Spl (Ballhaus *et al.*, 1991), (4) Ol-Cpx (Ai, 1994), (5) Grt-Spl (Perchuk, 1991) thermometers, and (6) Grt-Opx thermobarometer (Aranovich and Berman, 1997) (Figure 4.3a and b).

For the spinel herzolite xenolith (*Ng07*), the Grt-Cpx and Grt-Opx intersect gives the lowest constraint at about 775°C and 8.5 kb (~28 km at 3.3 km/kb), while the Grt-Spl and Grt-Opx intersect suggests the highest constraint up to about 1,500°C and 33.5 kb (~110 km). The Ol-Cpx and Grt-Opx intersect provides the intermediate range of constraint about 1,100-1,125°C and 18.5-21 kb (~50-56 km) and the best-fit constraint value of 1,100°C and 18.5 kb.
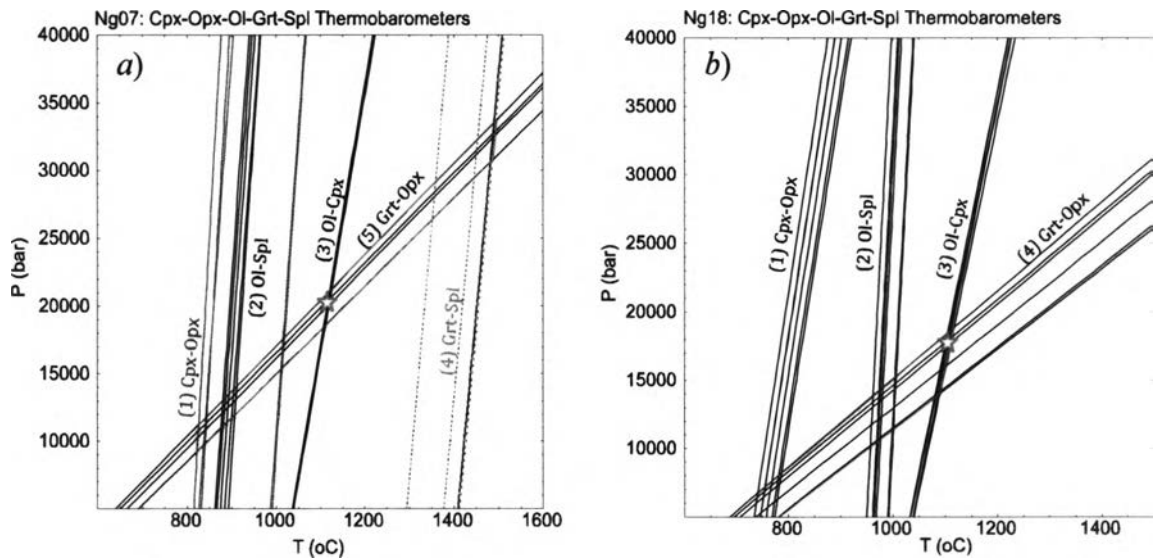

Figure 4.3 *a*) P-T constraints of spinel lherzolite, *Ng07*, according to 5 different thermo-barometers including (1) Cpx-Opx (Brey and Köhler, 1990), (2) Ol-Spl (Ballhaus *et al.*,1991), (3) Ol-Cpx (Ai, 1994) and (4) Grt-Spl (Perchuk, 1991) thermometers, and (5) Grt-Opx thermobarometer (Aranovich and Berman, 1997). Star symbol marking the best-fit P-T condition within the constraint area.
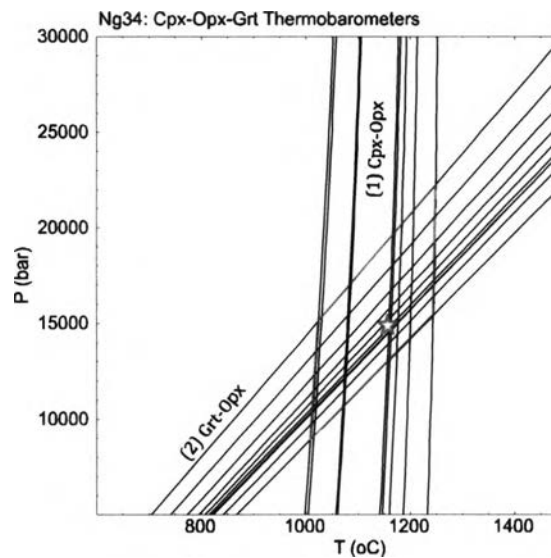
b) P-T constraints of spinel wehrlite, *Ng18*, according to 4 different thermo-barometers including (1) Cpx-Opx (Brey and Köhler, 1990), (2) Ol-Spl (Ballhaus *et al.*, 1991) and (3) Ol-Cpx (Ai, 1994) thermometers, and (4) Grt-Opx thermobarometer (Aranovich and Berman, 1997). Star symbol marking the best-fit P-T condition within the constraint area.

For the spinel wehrlite xenolith (*Ng18*), the lowest constraint given by the Cpx-Opx and Grt-Opx intersect is at about 750°C and 7 kb (~23 km). The Ol-Spl and Grt-Opx intersect provides the intermediate range of constraint about 950-1,000°C and 10-15.5 kb (~33-50 km). The highest constraint given by the Ol-Cpx and Grt-Opx intersect suggests up to about 1,100°C and 18.5 kb (~60 km), which also represent

the best-fit constraint for this sample. In this sample, the Grt-Ol thermometer does not provide reasonable calculation results.

Pyroxenite Xenoliths: The P-T constraints of this xenolith group were obtained from one representative sample, *Ng34* (webterite; Figure 4.4). Because of only 3 mineral phases observed, e.g. orthopyroxene, clinopyroxene and kelyphitic garnet, two geothermobarometers, which are (1) Cpx-Opx thermometer (Brey and Köhler, 1990) and (2) Grt-Opx thermobarometer (Aranovich and Berman, 1997), were applied to constraint a PT condition. From the intersecting area between the Cpx-Opx and Grt-Opx, the lowest limit is at about 1,000°C and 9 kb (~30 km at 3.3 km/kb) and the highest is up to about 1,200°C and 22.5 kb (~74 km). The intermediate range of constraint is about 1,075-1,090°C and 10.5-17 kb (~35-56 km).

Figure 4.4 P-T constraints of spinel-free websterite, *Ng34*, according to 2 different thermobarometers including (1) Cpx-Opx thermometer (Brey and Köhler, 1990) and (2) Grt-Opx thermobarometer (Aranovich and Berman, 1997). Star symbol marking the best-fit P-T condition within the constraint area.

Mafic granulite Xenoliths: The P-T constraints of this xenolith group were obtained from 3 representative samples. *KNt01* sample, which contains the most complete mineral assemblage available for P-T calculation, is a representative for the

foliated corundum-bearing mafic granulite variety (Figure 4.5a). *Ng21* sample represents the composite banded variety (Figure 4.5b). *KMb01* sample, which is the most felsic (anorthositic) composition in this study, represents the non-foliated corundum-free variety (Figure 4.6).
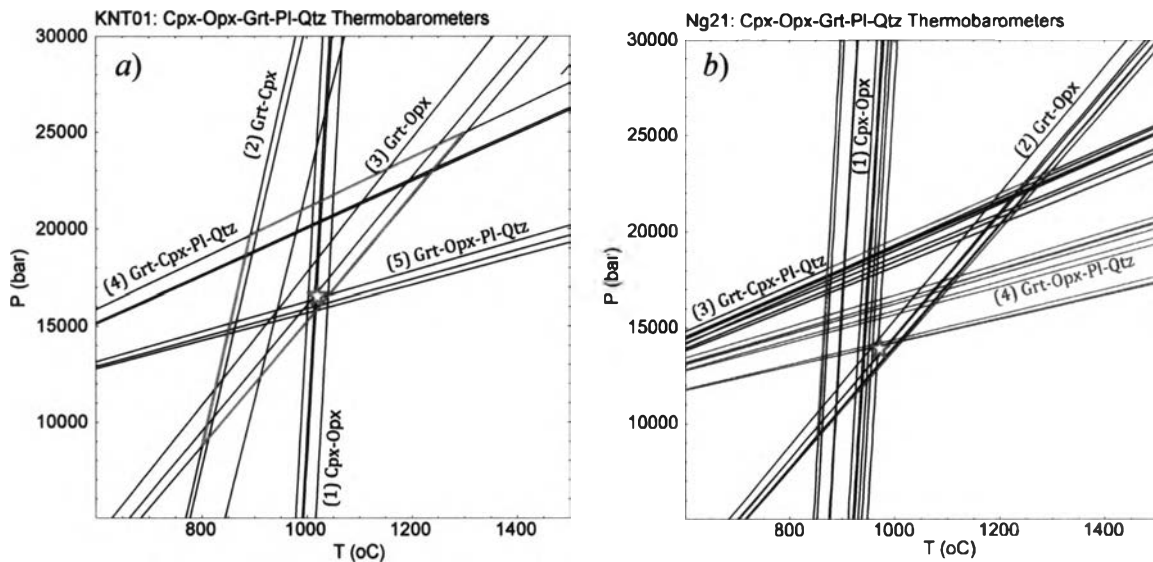

Figure 4.5 *a*) P-T constraints of foliated mafic granulite, *KNt01*, according to 5 different thermobarometers including (1) Cpx-Opx (Brey and Köhler, 1990), (2) Grt-Cpx (Ai, 1994) and (3) Grt-Opx (Aranovich and Berman, 1997) thermometers, and (4) Grt-Cpx-Pl-Qtz (Eckert *et al.*, 1991) and (5) Grt-Opx-Pl-Qtz (Lal, 1993) barometers. Star symbol marking the best-fit P-T condition within the constraint area.
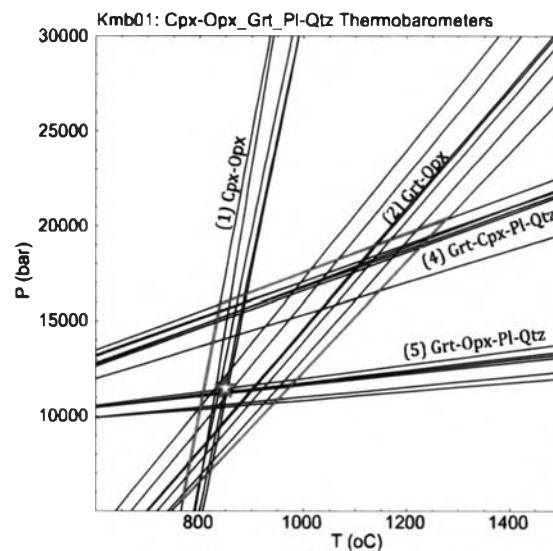
  b) P-T constraints of banded mafic granulite, *Ng21*, according to 4 different thermobarometers including (1) Cpx-Opx (Brey and Köhler, 1990) and (2) Grt-Opx (Aranovich and Berman, 1997) thermometers, and (3) Grt-Cpx-Pl-Qtz (Eckert *et al.*, 1991) and (4) Grt-Opx-Pl-Qtz (Lal, 1993) barometers. Star symbol marking the best-fit P-T condition within the constraint area.

For the corundum-bearing mafic granulite xenoliths (*KNt01* and *Ng21*), the Grt-Cpx and Grt-Opx intersect gives the lowest constraint at about 800°C and 8.7 kb (~29 km at 3.3 km/kb), while the Grt-Opx and Grt-Cpx-Pl-Qtz intersect yields the highest constraint up to about 1300°C and 23 kb (~76 km). The Cpx-Opx, Grt-Opx-Pl-Qtz and Grt-Cpx-Pl-Qtz intersects confine the intermediate range of constraint about 875-975°C and 13.5-19.5 kb (~45-65 km). The Cpx-Opx, Grt-Opx and Grt-Opx-Pl-Qtz

intersect provides the best-fit P-T constraint at about 1,000°C and 16 kb (~53 km) for the foliated mafic granulite and 950°C and 14 kb (~46 km) for the composite banded one.

For the corundum-free granulite xenolith (*KMb01*), the lowest constraint given by the Cpx-Opx and Grt-Opx intersect is at about 750°C and 5.5 kb (~18 km) while the highest constraint by the Grt-Spl and Grt-Opx intersect suggests up to about 1275°C and 20.5 kb (~68 km). The Cpx-Opx, Grt-Opx and Grt-Opx-Pl-Qtz intersect provides the best-fit P-T constraint at about 850°C and 11 kb (~36 km) that fall within the intermediate range of constraint (900-950oC and 11-19 kb).

Figure 4.6 P-T constraints of felsic granulite, *KMb01*, according to 4 different thermobarometers including (1) Cpx-Opx (Brey and Köhler, 1990) and (2) Grt-Opx (Aranovich and Berman, 1997) thermometers, and (3) Grt-Cpx-Pl-Qtz (Eckert *et al.*, 1991) and (4) Grt-Opx-Pl-Qtz (Lal, 1993) barometers. Star symbol marking the best-fit P-T condition within the constraint area.

In conclusion, the xenoliths of the peridotite group have an equilibrium P-T range of 750-1500°C and 7-33.5 kb (~23-110 km). The best P-T constraint of this group is likely ~ 1100°C and 18.5 kb, about 61 km depth equivalent. The websterite was equilibrated within the range of ~1000-1200°C and 9-22.5 kb (30-74 km). The best estimated P-T constraint of this group is ~1075°C and 12.5 kb equivalent to

depth about 40 km. The P-T range of the corundum-bearing xenoliths is about 800-1300°C and 8.7-23 kb and 750-1275°C and 5.5-24 kb (18-68 km). Seemingly, the best retained equilibrium for corundum-bearing granulite sub-group is at depth about 50 km in range of 950-1000°C and 14-16 kb (~40-50 km) and for the corundum-free granulite recorded the equilibration constraint at 850°C and 11 kb or at depth less than 40 km.

Therefore, the results of thermobarometric estimation imply that all the xenoliths were achieved their closure equilibria P-T constraints under a range of lower crust-upper mantle condition. The peridotite xenoliths were formed at deepest depth in the upper mantle region. The corundum-bearing xenoliths were also created within the upper mantle, but at a shallower level closer to the Moho. The pyroxenite (e.g. spinel-free websterite) xenoliths were formed near the Moho zone, whereas the corundum-free granulite xenolith was formed at shallowest level above the Moho.

Psuedosections of Xenoliths: Based on bulk-rock analyses of the xenoliths, the expected mineral stability of each sample is calculated and graphically illustrated in a form of pseudosection diagram by using the PerPlex program set. The pseudosections of seven selected xenolith samples overlain by estimated P-T constrains from PET are shown in Figures 4.7-4.9.

Results: Mineral assemblages given by pseudosections generally agree well to those petrographically observed in the samples. In addition to main phases, e.g. clinopyroxene, orthopyroxene, plagioclase and garnet, kyanite is always shown as another stable phase in high P-T range in most samples. The appearance of the kyanite phase from the calculation suggests that the mineral assemblages of the xenoliths have been formed within the kyanite stability field and further ensures the RAMAN results on tiny Al_2SiO_5 rods within the plagioclase hosts to be kyanite rather than sillimanite. However, corundum phase, an essential minor phase in all crn-bearing samples, does not appear in most of calculated psuedosections, except in that of KNt02-1, of which the whole-rock chemical is obtained from a plagioclase dominated layer. This implies that corundum is rather not stable in such bulk

compositions. On the contrary, quartz, which normally observed in the most crn-bearing samples, is usually shown as a stable phase.
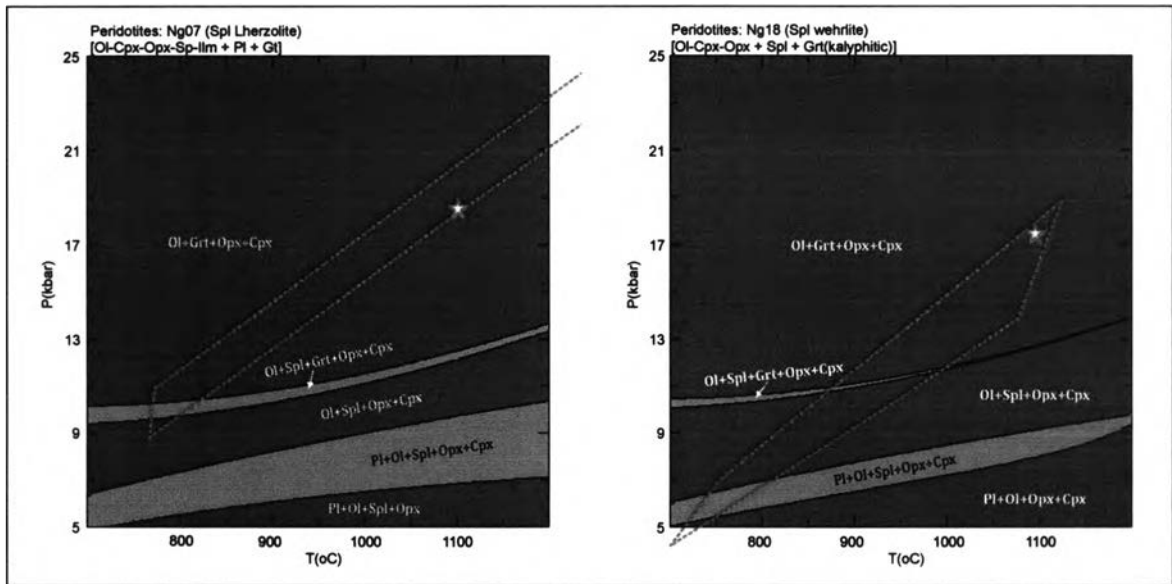

Figure 4.7 Pseudosection diagrams of the periditite xenoliths represented by Spl lherzolite (*Ng07*: left) and the Spl wehrlite (*Ng18*: right).
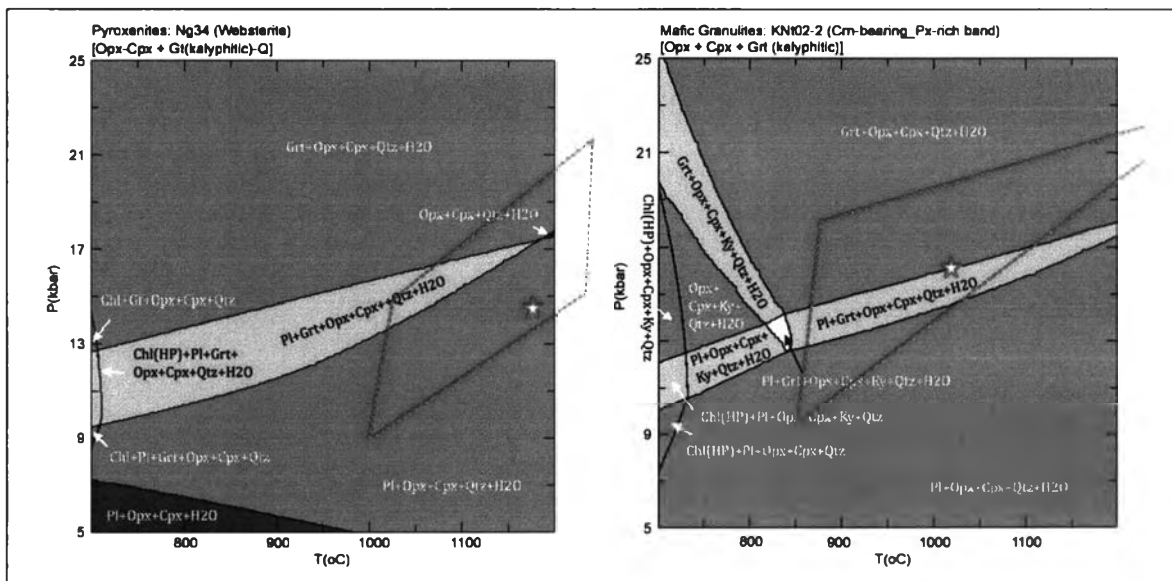

Figure 4.8 Pseudosection diagrams of the pyroxenite xenoliths represented by Spl-free websterite (*Ng34*: left) compared to the pyroxene-rich band of the crn-bearing granulite (*KNt02_2*: right).
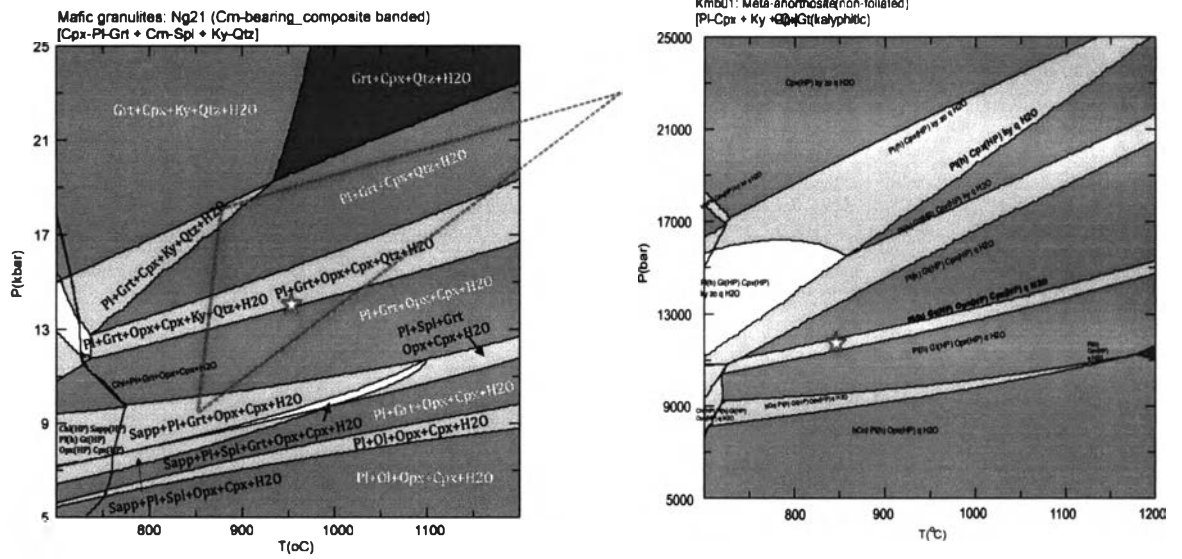
Figure 4.9 **Pseudosection diagrams of the granulite xenoliths represented by foliated, Crn-beaing mafic granulite (*Ng21*: left) compared to the crn-barren felsic granulite (*KMb01*: right).**